CORTEX 133 (2020) 358–370

Available online at www.sciencedirect.com

ScienceDirect

Journal homepage: www.elsevier.com/locate/cortex

Research Report

It's not all about looks: The role of object shape in parietal representations of manual tools

Karla Matić [a,c,*], Hans Op de Beeck [c] and Stefania Bracci [b,c,**]

[a] Max Planck School of Cognition, Max Planck Institute for Human Cognitive and Brain Sciences, Leipzig, Germany
[b] Center for Mind/Brain Sciences, University of Trento, Rovereto, Italy
[c] Brain and Cognition, Leuven Brain Institute, University of Leuven (KU Leuven), Leuven, Belgium

ARTICLE INFO

Article history:
Received 29 November 2019
Reviewed 3 March 2020
Revised 5 June 2020
Accepted 23 September 2020
Action editor Thomas Schenk
Published online 7 October 2020

Keywords:
Tools
Body-object interaction
MVPA
Representational similarity analysis
Dorsal visual stream

ABSTRACT

The ability to build and expertly manipulate manual tools sets humans apart from other animals. Watching images of manual tools has been shown to elicit a distinct pattern of neural activity in a network of parietal areas, assumingly because tools entail a potential for action—a unique feature related to their functional use and not shared with other manipulable objects. However, a question has been raised whether this selectivity reflects a processing of low-level visual properties—such as elongated shape that is idiosyncratic to most tool-objects—rather than action-specific features. To address this question, we created and behaviourally validated a stimulus set that dissociates objects that are manipulable and nonmanipulable, as well as objects with different degrees of body extension property (tools and non-tools), while controlling for object shape and low-level image properties. We tested the encoding of action-related features by investigating neural representations in two parietal regions of interest (intraparietal sulcus and superior parietal lobule) using functional MRI. Univariate differences between tools and non-tools were not observed when controlling for visual properties, but strong evidence for the action account was nevertheless revealed when using a multivariate approach. Overall, this study provides further evidence that the representational content in the dorsal visual stream reflects encoding of action-specific properties.

1. Introduction

The outstanding manual dexterity and capability of fine-motor coordination required for the use of manual tools renders humans unique among primates. Similarly to other evolutionary relevant categories—such as faces and bodies (for social interactions) and places (for spatial navigation)—the category of tools has been shown to activate a distinct

* *Corresponding author*. Max Planck School of Cognition, Max Planck Institute for Human Cognitive and Brain Sciences, Leipzig, Germany.
** *Corresponding author*. Center for Mind/Brain Sciences, University of Trento, Rovereto, Italy.
E-mail addresses: karla.matic@maxplanckschools.de (K. Matić), stefania.bracci@unitn.it (S. Bracci).
https://doi.org/10.1016/j.cortex.2020.09.016

network of brain areas. This tool-selective network comprises areas along the ventral (Bracci, Cavina-Pratesi, Ietswaart, Caramazza, & Peelen, 2012; Chao & Martin, 2000; Downing, Chan, Peelen, Dodds, & Kanwisher, 2006; Macdonald & Culham, 2015; Perini, Caramazza, & Peelen, 2014) and dorsal (Boronat et al., 2005; Chao, Haxby, & Martin, 1999; Hermsdörfer, Terlinden, Mühlau, Goldenberg, & Wohlschläger, 2007; Kastner, Chen, Jeong, & Mruczek, 2017; Mruczek, von Loga, & Kastner, 2013; Peeters et al., 2009; Valyear, Cavina-Pratesi, Stiglick, & Culham, 2007) visual streams.

The critical role of these brain regions in processing tool knowledge and use is supported by evidence from lesion studies. These studies report selective impairments in patients' ability to manipulate (Koski, Iacoboni, & Mazziotta, 2002; Leiguarda & Marsden, 2000; Randerath, Goldenberg, Spijkers, Li, & Hermsdörfer, 2010) or verbally identify tools (Damasio, Grabowski, Tranel, Hichwa, & Damasio, 1996; Tranel, Damasio, & Damasio, 1997), in cases where the ability to manipulate or name other objects (e.g., chairs or animals) is left intact (for a review, see Johnson-Frey, 2004). A converging body of neuroimaging literature further corroborates these neurophysiological findings. While tool-selective areas are reported in the ventral object-recognition pathway (Beauchamp & Martin, 2007; Bracci, Cavina-Pratesi, Connolly, & Ietswaart, 2016; Chao et al., 1999), organization of the areas in the dorsal stream reflects functional support for tool-specific actions (Bracci & Op de Beeck, 2016; Brandi, Wohlschläger, Sorg, & Hermsdörfer, 2014; Gallivan, Adam McLean, Valyear, & Culham, 2013; Lewis, 2006). Importantly, even though parietal areas also encode information about graspability (Almeida, Mahon, & Caramazza, 2010; Konen & Kastner, 2008), and dorsal tool-selectivity has been suspected to solely reflect the areas' preferences for graspable features (Creem-Regehr & Lee, 2005), this has been refuted with various neuroimaging designs (e.g., Brandi et al., 2014; Mruczek et al., 2013; Valyear et al., 2007) and clinical studies (e.g., Randerath et al., 2010). Overall, it has been repeatedly shown that parietal areas encode grasp-related properties common to all manipulable objects separately from the idiosyncratic tool-specific action-related features (Brandi et al., 2014; Chen, Snow, Culham, & Goodale, 2017; Lewis, 2006; Valyear et al., 2007).

However, a debate has recently arisen as to whether this selectivity for tools is attributable to the proposed action properties, or if it rather reflects a plain selectivity for visual features (Sakuraba, Sakai, Yamanaka, Yokosawa, & Hirayama, 2012). Analogously to the recently renewed debate in object vision (Rice, Watson, Hartley, & Andrews, 2014; Watson, Hartley, & Andrews, 2014; Bracci et al., 2016; Proklova, Kaiser, & Peelen, 2016), it is possible that the observed neural effects for tools do not reflect the abstract property of category membership, but rather the visual properties that correlate highly with stimulus category—in this case, the distinct, elongated shape shared by most tool-objects (Almeida et al., 2014). This shape-based hypothesis was initially tested by Sakuraba et al. (2012), who found that elongated objects (e.g., an elongated vegetable) activated the alleged tool-related dorsal substrates. However, recent work by Chen et al. (2017) examined the shape-based account in more detail, and concluded that parietal areas process both object shape and action-related properties.

More generally, the long-prevailing notion of the dorsal pathway strictly supporting "vision-for-action" computations has recently been challenged from different perspectives. Accumulating evidence shows that the dorsal stream extracts features such as colour, size or shape (e.g., Freud, Culham, Plaut, & Behrmann, 2017; Konen et al., 2008) to support "vision-for-perception" that are independent of those generated in the ventral stream (Freud, Ganel, Shelef, Hammer, Avidan, & Behrmann, 2017). Parietal areas have also been shown to encode visual information adaptively, in accordance with the task requirements and behavioural goals (Xu, 2018; Bracci, Daniels, & Op de Beeck, 2017). Taken together, this undermines the established notion that object representations in parietal cortex are primary in the service of action; a more the general purpose of these representations might be to support behavioural goals, including both action and perception.

To test if object representational content in parietal cortex reflects action-specific properties *per se*, here we created and behaviourally validated a stimulus set that eliminates the effect of visual features, including object shape (Fig. 1), and delineates between objects that are a) manipulable and nonmanipulable (graspability control); and b) having different degrees of body-extension property (tool-hand effect). More specifically, manual tools are defined as extensors of the internal body schema when used to manually operate on other objects (Kastner et al., 2017); for example, when using a hammer to pound a nail, the hammer is functionally extending the boundaries of the hand by inducing changes to the body-schema (Maravita & Iriki, 2004). The degree of perceived body extension—how much an object is physically and functionally extending the body's boundaries (Bracci & Peelen, 2013)—is used here as a data-driven definition of tool-objects. By orthogonally manipulating object shape across object categories with different action components, this study allowed us to fully disentangle the action- and shape-related object representations, and examine the independent contribution of action-related properties to dorsal stream representational content.

2. Materials and Methods

2.1. Participants

For the fMRI study, 17 right-handed healthy volunteers with normal or corrected-to-normal vision ($M_{age} = 28$, $SD_{age} = 7.1$, 10 females) were recruited. No participants were excluded, but due to technical issues a total of 5 runs were excluded (in 2 participants). For the behavioural validation, 9 healthy volunteers (mean age 25 [SD 3.1], 5 females) were recruited. Decisions about the total number of participants were taken prior to data collection and were based on results from previous experimental protocols (e.g., Bracci, Daniels, & Op de Beeck, 2017). The procedures were approved by the medical ethical committee of the University of Leuven.

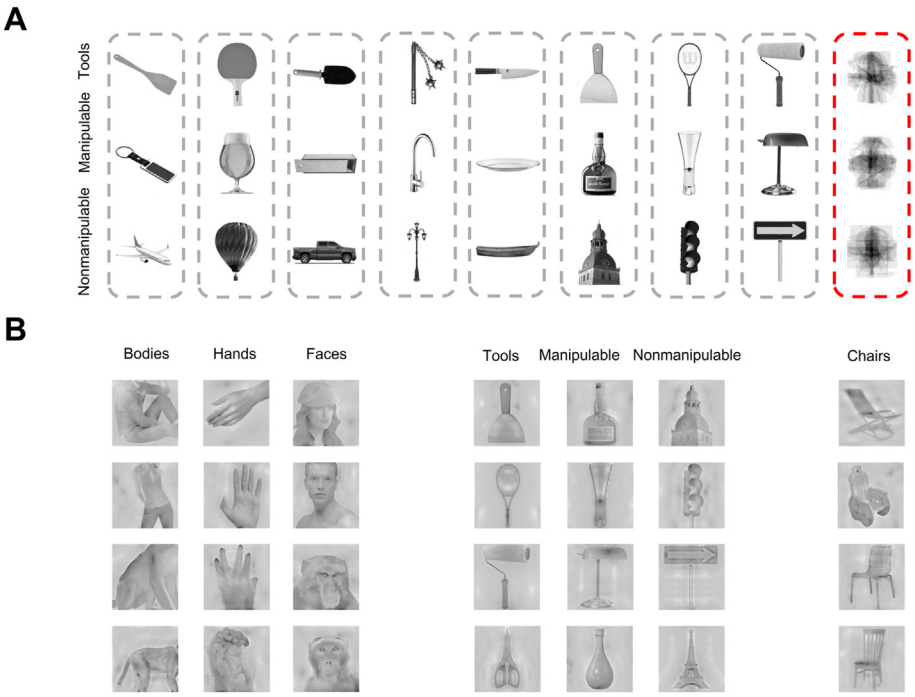

Fig. 1 – Stimulus set. A) Example images used for behavioural ratings. The stimulus set comprised a total of 72 images divided into 3 object categories: tools, manipulable objects, and nonmanipulable objects. Analysis of image shape low-level properties confirmed that the three object categories could not be distinguished based on their physical shape ($p > .05$ for all comparisons; last column: darker shade represents higher overlap). B) Example images used in the fMRI experiment; the stimulus set comprised a total of 168 images: three body categories (bodies, hands, faces), three object categories (same as in the behavioural experiment: tools, manipulable objects, nonmanipulable objects), and chairs as control condition. Images in the fMRI experiment were presented as showed here: in black-and-white, and controlled for spatial frequency and luminance (SHINE toolbox; Willenbockel et al., 2010).

2.2. *Behavioural validation*

Prior to the fMRI study, similarity judgements (Kriegeskorte & Mur, 2012) were used to validate the object stimulus set comprising 3 categories (tools, manipulable objects, and nonmanipulable objects), each consisting of 24 images (Fig. 1A). The purpose of this test was to verify that object conditions a) could not be distinguished based on perceived object shape; and b) could nevertheless be distinguished based on differential manipulability and tool-specific (body extension) properties. Three object dimensions were tested: visual similarity, object manipulability, and body extension.

The visual dimension was included to confirm that object categories could not be distinguished based on shape. To evaluate this, participants were instructed to *"arrange the objects according to their shape similarity (regardless of object orientation)"*.

The manipulability dimension assessed similarities in object manipulability properties, thus distinguishing handheld objects (tools and manipulable objects) from large non-graspable objects (nonmanipulable objects). Participants were asked to *"arrange the objects according to the following statements: (1) This object is easy to pick up; (2) This object is designed specifically for being easily graspable by one or both hands"*.

The body extension dimension was included to distinguish tools from the remaining objects based on their body-extension properties. Instructions required participants to *"arrange the objects according to the following statements: (1) This object is like a physical extension of my hand or arm; after using it for a while it almost feels to become part of my body; (2) When I use this object, my hand/arm movements are directly controlling this object to physically act on another object or surface."*

The instructions for the manipulability and body extension dimensions followed the approach previously reported by Bracci and Peelen (2013). This procedure allowed us to separate tools from manipulable and nonmanipulable objects with a data-driven approach (based on action-effector and manipulability properties) rather than using an arbitrary definition of object categories.

2.2.1. *Analysis of behavioural data*

Behavioural ratings of perceived similarity between different tools, manipulable objects and nonmanipulable objects were tested against theoretical models with permutation tests (n = 100,000). Behavioural matrices were shuffled and correlated with theoretical models using a Mantel test function (Glerean et al., 2016). Three theoretical models were simulated (Fig. 3A): 1) the category model, assuming high within-category and low between-category similarity; 2) the manipulability model, assuming high

similarity between tools and manipulable objects relative to nonmanipulable objects; and 3) the extension model, assuming a separated cluster for tools relative to both manipulable and nonmanipulable objects. We expected that 1) the category model *should not* significantly predict the visual condition; 2) the manipulability model *should* significantly predict the manipulability condition; and 3) the extension model *should* significantly predict the ratings in the extension condition.

2.3. Acquisition of neural data

2.3.1. Stimulus set

Seven categories of objects were included in a block-design fMRI experiment. In addition to the three object categories validated with behavioural judgements (i.e., tools, manipulable objects, and nonmanipulable objects), the stimulus set comprised three categories of different body parts: bodies (only torso; without the head, hands and feet), hands, and faces. These conditions were included to test representational similarities between objects and body parts that differ in action properties. For example, hands and bodies were found to differ in the ventral stream, where viewpoint-invariant grasp information was revealed in the hand-selective voxels, but not in nearby body-selective voxels (Bracci, Caramazza, & Peelen, 2018). According to the action-based account, we expected to find a hand-tool effect (i.e., that objects with action-specific properties would cluster with hands but not with other body parts), and conversely, we expected hands to cluster with objects depending on their action-properties (i.e., more closely with tools and less closely with non-manipulable objects). For the body part conditions, half of the images depicted monkey body parts and the remaining half depicted human body parts (Fig. 1B); previous imaging research has shown that human and monkey body parts do not result in differential responses in human ventrotemporal cortex (Kriegeskorte, Mur, Ruff, et al., 2008). Finally, images of chairs were used as a control condition, as commonly done in fMRI studies investigating category selectivity (e.g., Downing, Jiang, Shuman, & Kanwisher, 2001).

Each condition consisted of 24 grayscale images (4° × 4°, 400 × 400 pixels) on a white background (Fig. 1B). In addition to behavioural validation for shape and action-related properties (i.e., manipulability and body extension), all images were controlled for low-level visual properties (e.g., spatial frequencies and luminance) by means of the SHINE toolbox (Willenbockel et al., 2010), thus ensuring that low-level image properties were not differentially correlated with category membership.

2.3.2. Scanning procedure

The fMRI study consisted of two separated sessions, each performed on a different day (constrained by a maximum of one week between sessions). The data from each subject was collected simultaneously with the data for another study (not reported here). For the present study, we collected 4 runs per scanning session, resulting in 8 runs in total. Each run lasted 408 sec (204 volumes). In the middle of the scanning session, an anatomical scan was collected. Each image was presented for 1 sec, with no inter-stimulus interval, in blocks of 24 sec (i.e., 24 images per block). For each subject and for each run, a fully randomized sequence of all 7 conditions was repeated 2 times, with a fixation block of 24 sec at the beginning, in the middle (between sequences), and at the end of each run.

The presentation of stimuli was conducted with the Psychophysics Toolbox package (Brainard, 1997) in MATLAB (2018b) (The MathWorks). Images were projected onto a screen and shown to the participants through a mirror mounted on the head coil. Participants were instructed to fixate their gaze on the fixation cross in the middle of the screen and passively observe the images.

2.3.3. Imaging parameters

The data was collected using a 3T Philips scanner with 32-channel coil in the Department of Radiology of the University Hospital Leuven. MRI volumes were collected using echo planar (EPI) T2*-weighted sequence, with repetition time (TR) of 2s, echo time (TE) of 30 msec, flip angle (FA) of 90° and field of view of 216 mm. Each volume contained 37 axial slices, covering the whole brain, with matrix size of 72 × 72 and 3 × 3 × 3 mm voxel size. Anatomical images were acquired using the T1-weighted acquisition and MP-RAGE sequence, with a resolution of 1 × 1 × 1 mm.

2.4. Neural data analysis

2.4.1. Preprocessing

Preprocessing and data analysis were conducted using the Statistical Parametric Mapping software package (SPM12, Wellcome Trust Centre for Neuroimaging London) and MATLAB (R2018a, The MathWorks). Standard preprocessing steps were applied to functional images: spatial realignment (to the first image) to correct for head motion; slice-timing correction; coregistration of functional and anatomical images; normalisation to a Montreal Neurological Institute's ICBM152 template; and spatial smoothing by convolution with a Gaussian kernel of 4 mm FHM (Op de Beeck, 2010). Following the exclusion criterion defined prior to preprocessing, runs in which the head movement exceeded the size of one voxel (i.e., misalignment was larger than 3 mm) were excluded from subsequent analysis (altogether 5 runs in 2 subjects).

The preprocessed signal was then modelled for each voxel, in each participant, and for each of the 7 conditions using a general linear model (GLM). The GLM included regressors for each experimental condition (7 regressors of interest) and for 6 motion correction parameters (x, y, z for translation and rotation). The canonical haemodynamic response function was convolved with the boxcar function delineating the timepoints of presentation of experimental conditions to model each predictor's time course.

2.4.2. Regions of interest (ROIs)

Given the extensive evidence for the left hemispheric lateralization of the tool network (Lewis, 2006), two main ROIs were defined (Fig. 2A): left intraparietal sulcus (IPS) and left superior parietal lobule (SPL). The ROIs were defined at the group level with a combination of anatomical and functional criteria. More specifically, each ROI was localized at the group level by selecting all active voxels revealed by the contrast 'all

categories' > 'baseline' and restricted to cytoarchitectonic probabilistic masks using Anatomy SPM toolbox v3.0 (Eickhoff et al., 2007; IPS was defined as areas hIP1-hIP8; SPL was defined as 5L, 5M, 5Ci, 7A, 7 PC, 7M, 7P). Based on previous studies that found a representational gradient within IPS for shape and action properties (Freud, Culham, et al., 2017; Mrcuzek et al., 2013), we further subdivided our main ROI IPS into its anterior (aIPS) and posterior (pIPS) sub-regions (aIPS comprising areas hIP1-hIP3, Choi et al., 2006; pIPS comprising areas hIP4-hIP8, Richter et al., 2019; Fig. 2B). This approach of using cytoarchitectonically defined ROIs allowed us to perform a dedicated assessment of structure–function relationships in the prominent regions of the dorsal visual stream.

2.4.3. *Multi-voxel pattern analysis*

To examine whether the pattern of neural response in parietal areas encodes tool-specific action-related property independently of shape properties, we employed correlation-based multi-voxel pattern analysis (MVPA; Haxby et al., 2001). For each ROI and sub-ROI, we first extracted the parameter estimates ("responses") for each voxel and for each condition (relative to baseline), and normalised per run by subtracting the mean response across all conditions. The dataset was then divided into two independent subsets, and the patterns of voxel activity associated with each condition in one subset were correlated with the patterns of voxel activity for each condition in the other subset (i.e., split-half cross-validation). This procedure was repeated 100 times, and correlations were averaged across all 100 correlations. For each ROI, this resulted in a 6×6 matrix of correlations reflecting the similarities between multivoxel patterns of activity for each condition pair. The control condition (chairs), whose purpose was to be used as contrast in univariate analyses, was excluded from this analysis because it was not controlled for shape. Correlation matrices were averaged across the upper and lower half and only the upper triangle (without diagonal values) of the resulting symmetric matrix was used as input for subsequent analyses. Resulting correlation values were Fisher transformed prior to statistical analyses.

To test the experimental hypothesis, a repeated-measures analysis of variance (ANOVA) was fitted using IBM SPSS Statistics v.25 (IBMCorp, 2013). The effect sizes were estimated by computing partial η^2 coefficients. Pairwise two-tailed *t*-tests were employed for post hoc analyses. Hedges' *g* for dependent measures, interpreted similarly as Cohen's *d* but recommended for small samples (Ellis, 2010), was calculated as an estimate of *t*-test effect size, using the 'Measures of Effect Sizes (MES)' Toolbox v.1.6 in MATLAB (Hentschke & Stüttgen, 2011).

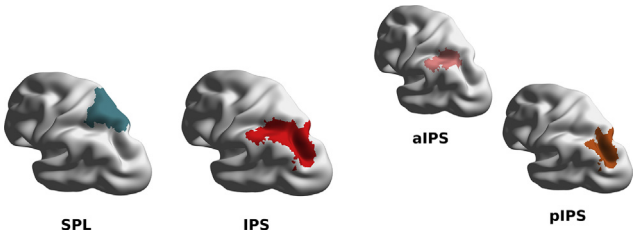

Fig. 2 – Regions of interest (ROIs). A.) Main ROIs: intraparietal sulcus (IPS) and superior parietal lobule (SPL). B) Sub-ROIs: anterior intraparietal sulcus (aIPS) and posterior intraparietal sulcus (pIPS). All ROIs were defined with a combination of functional (all conditions > baseline) and anatomical (masks) criteria.

2.4.4. *Multidimensional scaling (MDS)*

For visualization purposes, multidimensional scaling (MDS) was used to represent ROI's activity patterns in a two-dimensional space. To this end, for each ROI, the group averaged correlation matrix was first transformed into a dissimilarity matrix (1 minus correlation) and metric MDS was performed using the 'mdscale' MATLAB function. The resulting two-dimensional object arrangements were shown to facilitate the visualization of overall spatial relationships among response patterns of all experimental conditions.

2.4.5. *Materials availability and open access statement*

Experimental materials (including the stimulus set, behavioural data, neural dataset, and analysis code) can be accessed online at https://osf.io/yg9b4/. No part of the study procedures or analyses has been preregistered prior to the research being conducted. We report how we determined our sample size, all data exclusions, all inclusion/exclusion criteria, whether inclusion/exclusion criteria were established prior to data analysis, all manipulations, and all measures in the study.

3. Results

The aim of the present study was to test whether the previously reported tool selectivity in human parietal cortex (Chao & Martin, 2000; Kastner et al., 2017; Mruczek et al., 2013; Valyear et al., 2007) reflects the representation of tool-specific, action-related information, or can instead be fully explained by shape properties idiosyncratic to tools (e.g., Sakuraba et al., 2012). To this end, we constructed and behaviourally validated a stimulus set composed of object categories that differ in the domain of action properties (tools, manipulable objects, nonmanipulable objects), but are indistinguishable based on object shape and low-level visual properties (e.g., spatial frequency and luminance). We collected functional imaging data while participants passively observed images from object and body part categories in a block-design fMRI study.

3.1. *Behavioural validation*

To ensure that our stimulus set was optimally constructed to address our research question, the 3 object conditions (i.e., tools, manipulable and nonmanipulable objects) were first validated behaviourally; this validation aimed to confirm that objects are indistinguishable by shape, and that they entail a differential degree of action-related properties. Results confirmed these prerequisites. First, images across the three object categories were expected to be indistinguishable based on perceived shape (i.e., to be rated differently from the category model; Fig. 3A, left). A permutation test confirmed this criterion: as clearly observable by visual inspection of the

behavioural data (Fig. 3B, left), shape ratings were not significantly correlated with the category model ($r = .14$, $p = .5839$).

Second, tools and manipulable objects should be judged similarly with respect to manipulability properties, relative to nonmanipulable objects. A permutation test confirmed this criterion, in line with the clearly visible pattern of similarity between behavioural ratings on object manipulability (Fig. 3B, middle) and its hypothetical model (Fig. 3A, middle); that is, the manipulability model significantly predicted behavioural ratings on object-grasping properties ($r = .91$, $p < .001$). Even though the alternative action model (extension model) also predicted the behavioural ratings on object-grasping properties ($r = .24$, $p = .006$), the manipulability model was shown to perform significantly better ($p < .001$). In other words, images of tools and manipulable objects were conclusively judged to be similarly graspable relative to nonmanipulable objects, hence confirming the object manipulability criterion.

Third, the body extension dimension should predict differential ratings for tools relative to other manipulable objects and nonmanipulable objects. The definition of tools employed in the present study assumes that tools are all objects that can be considered a direct extension of a person's hand when physically acting on another object or surface (Maravita & Iriki, 2004). Similarly to tools, manipulable objects might, to a certain degree, be associated with hand actions as well (e.g., door handle), but in contrast to tools they are not expected to extend to body representations. As predicted, the permutation test confirmed that the extension model significantly predicts body extension ratings (Fig. 3A, B right; $r = .72$, $p < .001$). Importantly, the extension model significantly overtook the alternative manipulability model ($p < .05$), despite the latter explaining the extension ratings above chance ($r = .62$, $p < .001$). The tool-items, as compared to other manipulable objects, were therefore validated as being objects that extend the body's acting space, thus providing a data-driven definition of tools.

3.2. *Functional MRI study*

3.2.1. *No univariate tool selectivity in parietal cortex*

A standard second-level univariate analysis was conducted to examine the selectivity for tools in the parietal cortex. Contrary to previous studies reporting selectivity for tools in IPS and SPL, no significant activations were found when contrasting responses for tools against manipulable objects, nonmanipulable objects, or even chairs ($p_{uncorrected} = .001$). Similar results were observed even at a less conservative threshold ($p_{uncorrected} = .01$) and when contrasts were tested separately in each individual subject.

One possible explanation for this result is that previously reported parietal activations were not driven by a tool-specific action property; they might rather be driven by object visual features (e.g., elongated shape) as earlier proposed by Sakuraba et al. (2012), or low-level properties (e.g., spatial frequencies) which have been argued to drive object cortical organization (Rice et al., 2014). Since our stimulus set was orthogonally controlled for object shape and matched for low-

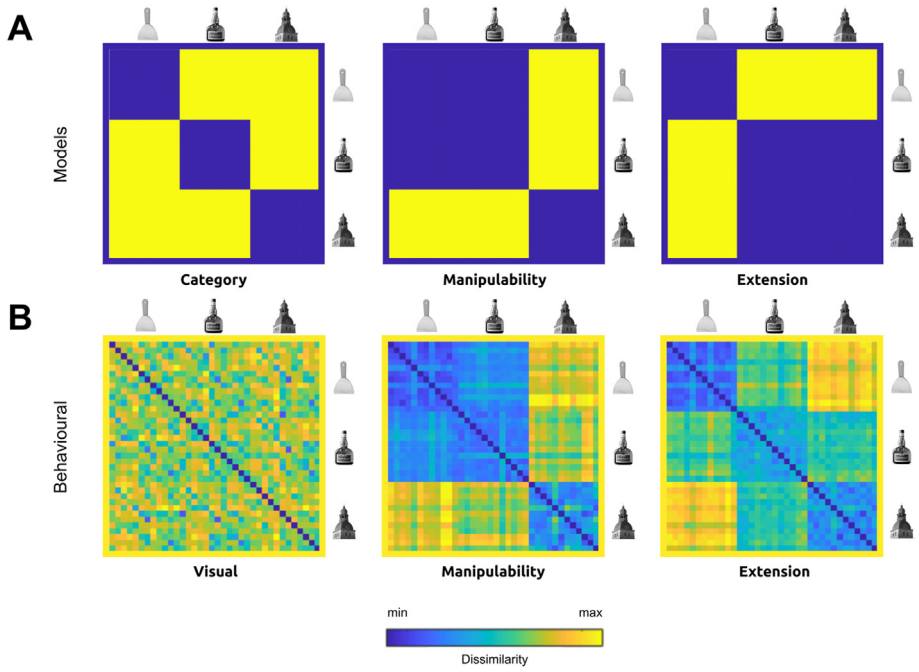

Fig. 3 – Hypothetical models and mean dissimilarity matrices for behavioural ratings. A) The three models are visualized: The category model assumes high within-category and low between-category similarity (left); the manipulability model assumes high similarity between tools and manipulable objects relative to nonmanipulable objects (middle); and the extension model assumes a separate cluster for tools relative to both manipulable and nonmanipulable objects (right). B) The dissimilarity matrices (1 minus correlation) are shown for behavioural ratings (visual, object manipulability, and body extension). For each object dimension, each cell in the matrix shows the average similarity judgements for a given object pair. Blue represents higher similarity between images.

level visual properties, this lack of tool selectivity could be in accordance with one of these alternative hypotheses. To investigate this possibility, we further tested the action-based account by means of more powerful multi-voxel pattern analyses.

3.2.2. *Action-specific multivariate representations in parietal cortex*

By means of MVPA, dimensions underlying object representations can be inferred from the analysis of response patterns' similarities for different experimental conditions. In light of our main question, two contrasting predictions can be made about parietal cortex representations. The *action-based account* predicts higher similarity between activation patterns for tools and hands relative to other objects or body parts, thus highlighting a common action effector role for hands and tools (Bracci & Peelen, 2013). Conversely, the *shape-based account*, which suggests that previously reported tool-selectivity in parietal cortex reflects solely object shape (as proposed by Sakuraba et al., 2012), predicts similar activation patterns for all object categories in a shape-controlled stimulus set. Finally, based on previous results (e.g., Cavina-Pratesi et al., 2010; Mruczek et al., 2013), we might expect different results in parietal areas IPS and SPL; that is, object action-related properties might be represented differently in IPS and SPL.

We conducted correlational MVPA separately in left IPS and SPL. Correlational matrices (Fig. 4A) show correlations between patterns of neural activity for the 6 experimental conditions after averaging results across participants. Higher correlations (red) represent a more similar pattern of activation for two conditions, and hence more similar neural representations. To test our experimental hypothesis, we conducted a 2 × 3 × 3 ANOVA with ROI (IPS and SPL), Object (tools, manipulable, and nonmanipulable) and Body (bodies, hands, faces) as within-subject predictors, and the observed correlations between multi-voxel patterns of neural activity per subject as dependent variables.

Results (Table 1) revealed no significant main effect of ROI ($F_{1.,16} = .01$, $p = .973$, $\eta^2 = .00$), thus suggesting no overall difference between representations of body-parts and objects with different action-related properties in IPS and SPL. Additionally, a main effect of Body reached significance ($F_{2,32} = 4.81$, $p = .015$, $\eta^2 = .23$), as did the interaction between Body and Object ($F_{4,64} = 5.03$, $p = .003$, $\eta^2 = .24$), showing that observed patterns of neural activity for the different body parts correlate differentially with representations of objects that convey different action properties. The interaction of interest (Body x Object) was further investigated with post-hoc *t*-tests, after averaging results across the two ROIs.

Results (Table 2; Fig. 4C) revealed a significantly higher correlation between neural activation patterns for hands and tools than for hands and manipulable ($t_{16} = 2.97$, $p = .009$, $g = 1.16$) or hands and nonmanipulable objects ($t_{16} = 3.83$, $p = .002$, $g = 1.37$), and no difference between correlations of hands and manipulable compared to hands and nonmanipulable objects ($t_{16} = 1.31$; $p = .208$, $g = .39$). Additionally, tools were significantly more correlated with hands than other body parts: bodies ($t_{16} = 5.13$, $p = .0001$, $g = 1.76$) and faces ($t_{16} = 4.11$, $p = .0008$, $g = 1.67$). These parietal results replicate previously observed findings in the ventral stream for the special link between neural representations for action "effectors"—regardless of whether they are body effectors (hands) or object effectors (tools; Bracci & Peelen, 2013). In agreement with the left hemisphere computational dominance in action processing, the hand-tool effect was not observed in the right hemisphere. Hands were not significantly more correlated with tools relative to the other object conditions [hands-tools *vs* hands-manipulable: $t(16) = 1.59$, $p = .12$; hands-tools *vs* hands-nonmanipulable: $t(16) = 2.01$, $p = .06$].

The representational space in the two ROIs is visualized by means of multidimensional scaling (MDS; Fig. 4B). The MDS plots further support the above results; namely, that the representations of hands and tools are closely represented in the neural space, and that they are more proximal than representations of tools and other body parts, or hands and other objects. Together, these results provide evidence for the action-based account: even when most shape properties are controlled for, parietal areas IPS and SPL clearly represent tool-specific action properties.

3.2.3. *Differential object action properties in IPS and SPL*

We found no significant overall differences between the two ROIs, even though the literature points to an important role played by IPS in object grasping, which differentiates it from the preferential involvement of SPL in reaching movements (Cavina-Pratesi et al., 2010; Konen, Mruczek, Montoya, & Kastner, 2013). These computational differences predict differential representational similarity for the three object categories in IPS and SPL; the IPS is expected to encode graspable objects (tools and manipulable) similarly, and differently from non-graspable objects. This prediction was confirmed when examining the object-object correlations, as shown in Fig. 5.

Representational similarity between the two manipulable conditions (tools and manipulable objects) in the IPS is shown to be significantly larger than would be expected by chance ($t_{16} = 2.52$, $p < .05$), and significantly higher relative to correlations between the manipulable objects (including tools) and non-manipulable objects ($t_{16} = 2.29$, $p < .05$). In other words, in addition to the tool-specific effect, a grasping effect common to both tools and manipulable objects emerged in the IPS—in line with previous findings (Cavina-Pratesi et al., 2010; Culham & Valyear, 2006; Konen et al., 2013). The grasping effect was not observed in SPL, where there was no difference between the three object pairs (tools-manipulable *vs* tools-nonmanipulable: $t_{16} = .27$, $p = .77$; tools-manipulable *vs* manipulable-nonmanipulable: $t_{16} = 1.23$, $p = .24$; tools-nonmanipulable *vs* manipulable-nonmanipulable: $t_{16} = 1.02$, $p = .32$). These results support findings pointing to a differential role of IPS and SPL in object grasping (Cavina-Pratesi et al., 2010; Culham & Valyear, 2006; Konen et al., 2013; Macdonald & Culham, 2015; Mruczek et al., 2013).

3.2.4. *Representations across the anterior-posterior axis*

A recent proposal suggests a shape-action gradient in the dorsal stream, where posterior dorsal representations—in addition to the ventral ones—play a role in object perception by extracting object shape information and other perception-relevant properties (e.g., size and view-point invariance),

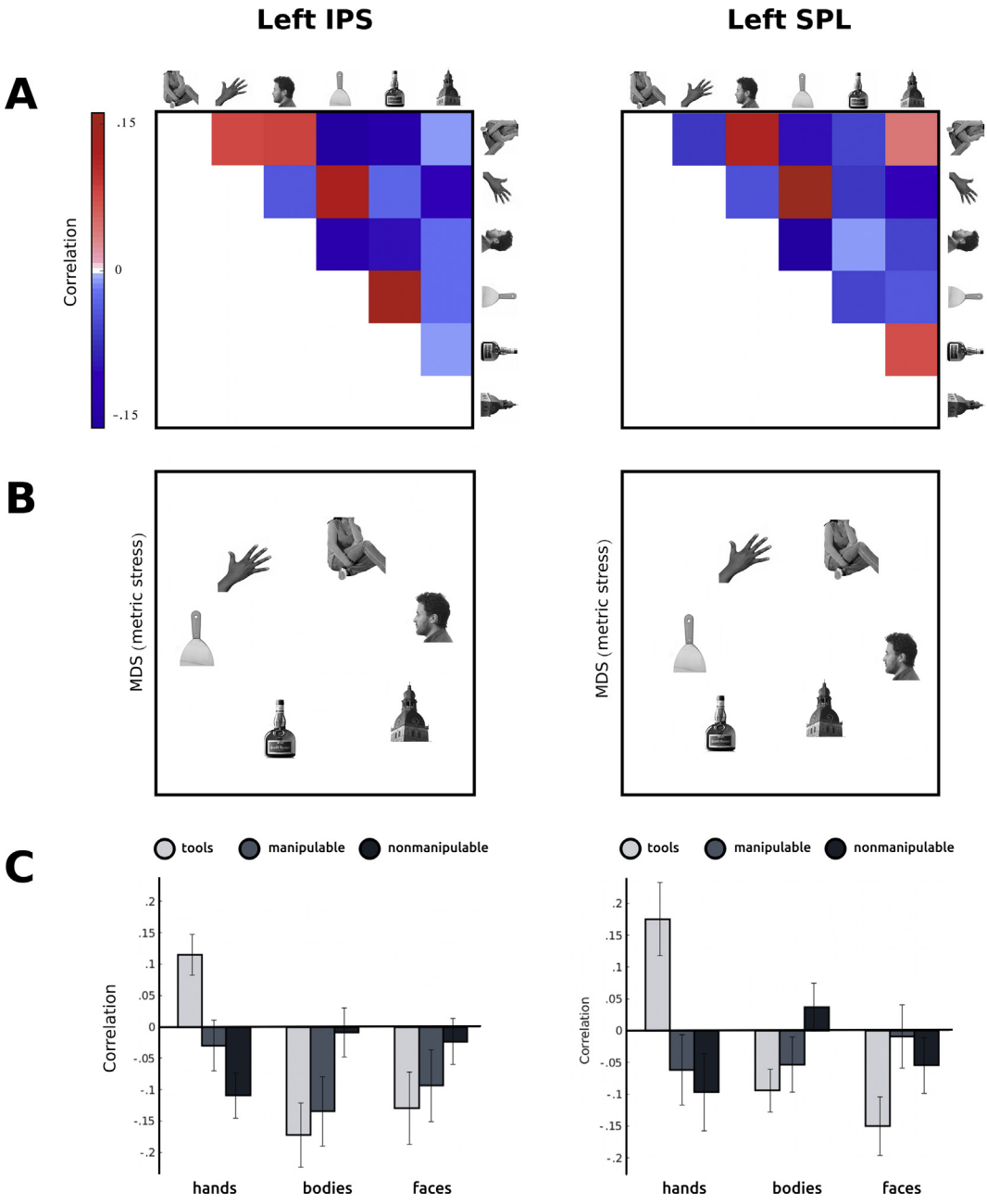

Fig. 4 – IPS (left) and SPL (right) representational space. A) Correlation matrices reflect similarities in patterns of voxel activity between condition pairs in IPS (left) and SPL (right); red reflects higher similarity. B) Representational space for the experimental conditions visualized by means of multidimensional scaling (MDS). Each icon represents the position of a condition in the representational space; the order in the left panel (counter-clockwise from top) is: hands, tools, manipulable, nonmanipulable, faces, and bodies. C) Mean correlations between patterns of voxel activity between object (tools, manipulable, nonmanipulable) and body (bodies, hands, faces) conditions are reported for IPS (left) and SPL (right) with standard error of the mean.

while the more anterior areas support visuomotor processing (Konen & Kastner, 2008; Freud, Culham, et al., 2017, Freud, Ganel, et al., 2017; Fabbri, Stubbs, Cusack, & Culham, 2017). To address whether different sub-regions within IPS show differential object encoding—with posterior IPS being less sensitive to action properties and more to object shape—we further investigated representations in anterior and posterior IPS (see Materials and Methods).

The results are reported in Fig. 6. Already by visual inspection, it is clear that representational similarities between objects and body parts do not qualitatively differ in anterior and posterior IPS. Statistical tests confirmed a strong coupling between hands and tools in both ROIs: hands were significantly more correlated to tools than to other objects ($t_{16} > 1.81$, $p < .05$, for all contrasts). Similarly, tools were significantly more correlated to hands than to other body parts ($t_{16} > 3.34$,

Table 1 – Repeated measures ANOVA with 3 within-subject predictors (ROI, Body, Object).

Source	df	Mean squares	F	p	Partial η^2
ROI	1	.000	.007	.937	.00
Body	2	.172	4.814	**.015**	.23
Object (*)	1.4	.009	.207	.739	.01
ROI × Body	2	.027	.836	.443	.05
ROI × Object (*)	1.7	.019	.916	.399	.05
Body × Object (*)	3.4	.403	5.034	**.003**	.24
ROI × Body × Object (*)	2.9	.054	1.023	.391	.06

Note. Partial η^2 = estimated effect size; (*) marks corrections for lack of homoscedasticity with Greenhouse-Geisser; highlighted in bold are $p < .05$.

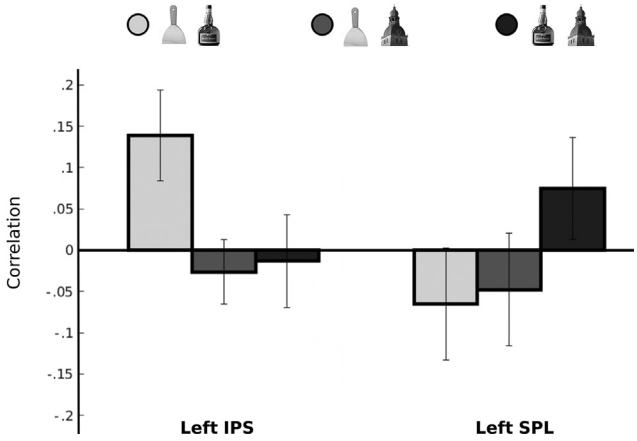

Fig. 5 – Representational patterns similarity for objects with different action properties. Mean correlations between patterns of voxel activity for the three object pairs (tools-manipulable, tools-nonmanipulable, and manipulable-nonmanipulable) reported for IPS (left) and SPL (right) with standard error of the mean.

$p < .001$, for all contrasts). These results show that parietal computations linked to hand-tool representational clustering may be extending throughout the whole intraparietal sulcus (but see Freud, Culham, et al., 2017, for discussion of functional segmentation of the IPS).

4. Discussion

Watching images of tools is known to elicit a distinct pattern of neural activity in parietal visual areas, assumingly because tools entail a potential for action—an idiosyncratic feature related to their functional use and not shared with other manipulable objects (Chao & Martin, 2000; Lewis, 2006; Valyear et al., 2007). However, recent reports (Almeida et al., 2014; Sakuraba et al., 2012) suggested that tool-related activity in the dorsal visual stream might be explained solely by object visual features—as tools are commonly of specific, elongated shape—rather than by their specific action-related features.

To test these competing hypotheses, we constructed a stimulus set orthogonally controlled for shape and low-level visual features, and consisting of tools, manipulable objects, and nonmanipulable objects. We investigated neural representations of those objects in dorsal visual stream. We found evidence in support of the action-based account; that is, at least in the conditions when no shape information is available, areas IPS and SPL in the dorsal visual stream extract tool-specific action-related features. We also observed differences between areas IPS and SPL; in line with previous research, we show that IPS, in addition to the tool-specific component, also encodes object-grasping properties common to manipulable objects (Cavina-Pratesi et al., 2010; Culham & Valyear, 2006; Konen et al., 2013; Macdonald & Culham, 2015; Mruczek et al., 2013). We discuss the specifics of these findings below.

4.1. *Evidence for the action-based account*

Results in both IPS and SPL revealed closely overlapping patterns of neural representations of hands and tools, as predicted by the action-based account. Notably, the activity pattern of hands did not correlate with other manipulable and nonmanipulable objects, and similarly, the activity pattern of tools did not correlate with other body parts (Fig. 4A, C). Our findings show high similarities for representations of action effectors, regardless of whether they are body parts (hands) or objects (tools). These findings dismiss the shape-based account, and provide additional evidence for the tight link between neural substrates for representations of hands and of those objects that extend the body's boundaries in object interaction (Bracci et al., 2012, 2016).

The observed overlap in representational patterns of hands and tools cannot be explained with the elongation hypothesis, which maintains that parietal tool-selectivity reflects solely the shape properties common to most tools (Sakuraba et al., 2012). Our stimulus set was orthogonally matched by shape

Table 2 – Pairwise comparisons of mean correlations between conditions.

Pairwise comparison	M_1 (SD_1)	M_2 (SD_2)	t	p	Hedges g (95% CI)
hands-tools vs					
hands-manipulable	.16 (.153)	−.02 (.148)	2.97	**.0092***	1.16 (.49, 1.95)
hands-nonmanipulable	.16 (.153)	.09 (.195)	3.83	**.0015****	1.37 (.74, 2.24)
bodies-tools	−.11 (.140)	.16 (.153)	5.13	**.0001*****	1.76 (1.02, 2.99)
faces-tools	−.12 (.165)	.16 (.153)	4.11	**.0008****	1.67 (.92, 2.81)
hands-manipulable vs					
hands-nonmanipulable	−.02 (.148)	.09 (.195)	1.31	.2082	.39 (−.18, 1.1)

Note. Tests that remained significant after correction for multiple comparisons (n = 5) are highlighted in bold; *$p < .01$; **$p < .001$; ***$p < .0001$.

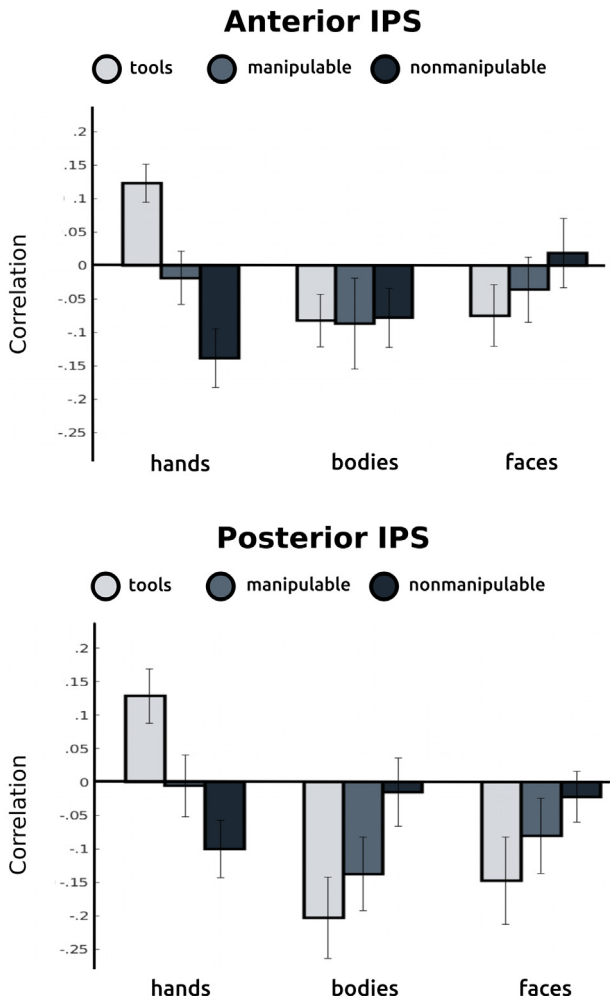

Fig. 6 – Anterior IPS (top) and Posterior IPS (bottom) representations. Mean correlations between patterns of voxel activity between object (tools, manipulable, nonmanipulable) and body (bodies, hands, faces) conditions are reported for aIPS (left) and pIPS (right) with standard error of the mean.

and controlled for low-level visual properties, and thus eliminated the contribution of visual features to neural activations. In such shape-controlled stimulus set, any observed difference in activation patterns between the three object categories (tools, manipulable objects, non-manipulable objects) would entail evidence against the strictly shape-based account. The evidence that the action-effector representational link between hands and tools did not extend to other objects or body parts shows that, when controlling for object shape and low-level visual features, parietal tool-selectivity cannot be explained by object visual properties only. This result is complementary to the findings of a recent study of Chen et al. (2017).

However, when using the standard univariate approach to localize tool-selective areas (against other manipulable or nonmanipulable objects, or even chairs), we observed no effect. While this is in misalignment with previous literature on tool selectivity (e.g., Kastner et al., 2017; Mruczek et al., 2013; Valyear et al., 2007), there are two plausible explanations. On the one hand, the lack of univariate selectivity might be due to the experimental choice to not use an active experimental task. Whereas some previous studies revealed tool-selective regions in IPS with univariate contrasts when using only passive observation (e.g., Chen et al., 2017), most of the previous findings of tool selectivity in parietal areas used not only an active task (e.g., one-back task), but even required participants to either imagine movements or pantomime the shown tools with overt movements (e.g., Choi et al., 2001; Moll et al., 2000; Rumiati et al., 2004). In addition, the attention of participants has been shown to be mediating the visual activations more strongly in parietal ROIs, as these regions do not respond as strongly to visual presentation as ventral areas (Fedorenko, Duncan, & Kanwisher, 2013). It is thus plausible that given our experimental design, the lack of univariate effects for tools can be ascribed to participants' decreased engagement.

On the other hand, lack of univariate selectivity for tools could be ascribed to our visually-controlled stimulus set: by eliminating the contribution of visual features, we may have eliminated the univariate selectivity, yet could still observe the representation of tool action-specific properties when using the more sensitive multivariate approach. This interpretation would suggest that both visual and action-related properties play a role in dorsal pathway representations; instead of being mutually exclusive, these properties may *both* be encoded in the areas of the dorsal visual stream, and potentially be mutually additive. In the conditions when no shape information is available, activations for tools in the dorsal areas may be weaker (reflected in the lack of univariate selectivity), but the tool-selective areas IPS and SPL can still extract the tool-specific information, relying on the action-related property (reflected in the overlapping representations of hands and tools).

4.2. *Tools and graspability: partially overlapping concepts*

Our results confirm previous reports (e.g., Cavina-Pratesi et al., 2010; Konen et al., 2013; Macdonald & Culham, 2015; Mruczek et al., 2013) that the overlap between hand and tool representations reflects a tool-specific property rather than only graspability affordances. If our ROIs were encoding graspability in general rather than action-specific properties in particular, correlations between activation patterns of hands and tools would not differ from the ones of hands and other manipulable objects; the only expected difference would be between manipulable and nonmanipulable objects. Since we found a significant difference between the relationships of hands-tools and hands-manipulable objects, and no difference between the relationship of hands with manipulable and nonmanipulable objects (Table 2; Fig. 4C), we conclude that parietal areas IPS and SPL encode action-related computations, specific to tools and not shared with other manipulable objects.

In addition to the tool-specific action effect, we also observed an overlap of at least some of the representations between tools and manipulable objects in the IPS (Fig. 5), which is in line with previous research (Konen et al., 2013;

Mruczek et al., 2013; Cavina-Pratesi, et al., 2010). Tools conceptually overlap with manipulable objects through the shared property of graspability, which we show both behaviourally (Fig. 3, 'Manipulability' model) and on a neural level in the IPS (Fig. 4, left side). Therefore, tool-related representations in the IPS can be thought of as a combination of their property of manipulability—overlapping with other manipulable but not with non-manipulable objects—*as well as* the action-specific property—characterised by the close overlap with the representations of hands—that is specifically related to the use of tools and not shared with other objects. In other words, representations of tools in the IPS include the concept of graspability, but the opposite is not true: the concept of manipulability may, but need not, include the tool-specific action property.

It is relevant to note that the non-manipulable objects in our stimulus set are objects of large real-life size. Whereas retinal size is controlled for in all three object conditions, physical size is, by definition, small for the two manipulable conditions and larger for non-manipulable objects. Therefore, another possible explanation for the observed effect of manipulability could be the imagined object size. The effect of the object real-size in parietal cortex has been investigated in the context of object affordances (using real objects) and limited to small graspable objects (Cavina-Pratesi, Goodale, & Culham, 2007; Fabbri et al., 2017; Kourtis, Vandemaele, & Vingerhoets, 2018). However, recent evidence suggests that properties we extract from objects vary depending on the viewing format: physical properties (e.g., object size, weight, elongation) are relevant when watching real 3D objects, but not 2D images (Holler, Fabbri, & Snow, 2020). Consolidating these findings, we conclude that the manipulability effect observed in IPS is unlikely to be explained by imagined object physical size. To comprehensively investigate the role of imagined object size in parietal cortex, future studies could test objects with different degrees of manipulability (high *vs* low), but similar real-life object size.

4.3. *Tool-specific properties across the anterior-posterior axis*

Another perspective on the question of whether—and how—action-related properties interact with shape representations comes from the studies proposing a hierarchical organisation of properties following an anterior-posterior gradient (e.g., Freud, Culham, et al., 2017; Freud, Ganel, et al., 2017; Konen & Kastner, 2008). This research suggests that object representations are not monolithic across the dorsal visual stream; rather, they are distributed hierarchically, with visual properties being encoded in the areas closer to the extrastriate visual cortex, and action-related properties in the anterior areas more proximal to the motor cortex. We investigated whether dorsal representations of tool-specific action properties follow a similar gradient by sub-dividing the ROI IPS into its anterior (aIPS) and posterior (pIPS) segments.

We found no anterior-posterior gradient in tool representations. The overlap of representations of hands and tools—implying an encoding of a tool-specific action-related property—was found to be almost identical in the aIPS and pIPS (Fig. 6). While this is in contrast to previous findings (Mruczek et al., 2013), our design notably differs in that it uses a stimulus set specifically designed to eliminate the effect of visual features. Thus, we provide evidence that areas of the dorsal visual stream extract action-related properties in the absence of distinct shape information.

Future directions and conclusion

The aim of the present study was to elucidate the role of visual- and action-related features on neural activations in the two most commonly reported tool-related parietal regions, IPS and SPL. We showed that, when controlling for visual features and manipulability, these two regions both elicit a distinct representational pattern for tool-specific, action-related features. This does not preclude the possibility that regions along the dorsal visual stream *also* encode visual properties (Freud, Culham, et al., 2017); however, given the use of a block design, the present study was unable to evaluate the representations of individual exemplars and thus the direct interaction between action and shape representations. Future research could utilise event-related designs to access the representations of individual exemplars and dissociate the effect of visual elongation *per se* on triggering action-related schemas.

Overall, while our results imply neither exclusiveness of tool-selectivity nor the pervasiveness of action-related organisation across parietal cortex, they do offer further evidence for the action-related account of object organisation in the dorsal visual stream.

Author contributions

Karla Matić: Conceptualization, Investigation, Data curation, Formal analysis, Visualization, Writing - original draft, Writing - review & editing.

Hans Op de Beeck: Conceptualization, Supervision, Funding acquisition, Writing - review & editing.

Stefania Bracci: Conceptualization, Methodology, Formal analysis, Supervision, Funding acquisition, Writing - review & editing.

Open practices

The study in this article earned Open Materials and Open Data badges for transparent practices. Materials and data for the study are available at https://osf.io/yg9b4/.

Acknowledgements

This work was supported by the FWO (Postdoctoral Fellowship 12S1317N and Research Grant 1505518N) to S.B., and the European Research Council (ERC Grant 2011-StG-284101), a federal research action (IUAP-P7/11), the KU Leuven Research Council (C14/16/031), Hercules Foundation grant ZW11_10, and an Excellence of Science Grant (G0E8718N) to H.O.B.

REFERENCES

Almeida, J., Mahon, B. Z., & Caramazza, A. (2010). The role of the dorsal visual processing stream in tool identification. *Psychological Science, 21*(6), 772–778.

Almeida, J., Mahon, B. Z., Zapater-Raberov, V., Dziuba, A., Cabaço, T., Marques, J. F., et al. (2014). Grasping with the eyes: The role of elongation in visual recognition of manipulable objects. *Cognitive, Affective & Behavioral Neuroscience, 14*(1), 319–335.

Beauchamp, M. S., & Martin, A. (2007). Grounding object concepts in perception and action: Evidence from fMRI studies of tools. *Cortex, 43*(3), 461–468.

Boronat, C. B., Buxbaum, L. J., Coslett, H. B., Tang, K., Saffran, E. M., Kimberg, D. Y., et al. (2005). Distinctions between manipulation and function knowledge of objects: Evidence from functional magnetic resonance imaging. *Cognitive Brain Research, 23*(2–3), 361–373.

Bracci, S., Caramazza, A., & Peelen, M. V. (2018). View-invariant representation of hand postures in the human lateral occipitotemporal cortex. *Neuroimage, 181*, 446–452.

Bracci, S., Cavina-Pratesi, C., Connolly, J. D., & Ietswaart, M. (2016). Representational content of occipitotemporal and parietal tool areas. *Neuropsychologia, 84*, 81–88.

Bracci, S., Cavina-Pratesi, C., Ietswaart, M., Caramazza, A., & Peelen, M. V. (2012). Closely overlapping responses to tools and hands in left lateral occipitotemporal cortex. *Journal of Neurophysiology, 107*(5), 1443–1456.

Bracci, S., Daniels, N., & Op de Beeck, H. (2017). Task context overrules object- and category-related representational content in the human parietal cortex. *Cerebral Cortex, 27*(1), 310–321.

Bracci, S., & Op de Beeck, H. (2016). Dissociations and associations between shape and category representations in the two visual pathways. *Journal of Neuroscience, 36*(2), 432–444.

Bracci, S., & Peelen, M. V. (2013). Body and object effectors: The organization of object representations in high-level visual cortex reflects body-object interactions. *Journal of Neuroscience, 33*(46), 18247–18258.

Brainard, D. H. (1997). The psychophysics toolbox. *Spatial Vision, 10*(4), 433–436.

Brandi, M. L., Wohlschläger, A., Sorg, C., & Hermsdörfer, J. (2014). The neural correlates of planning and executing actual tool use. *Journal of Neuroscience, 34*(39), 13183–13194.

Cavina-Pratesi, C., Goodale, M. A., & Culham, J. C. (2007). FMRI reveals a dissociation between grasping and perceiving the size of real 3D objects. *Plos One, 2*(5), e424.

Cavina-Pratesi, C., Monaco, S., Fattori, P., Galletti, C., McAdam, T. D., Quinlan, D. J., et al. (2010). Functional magnetic resonance imaging reveals the neural substrates of arm transport and grip formation in reach-to-grasp actions in humans. *Journal of Neuroscience, 30*(31), 10306–10323.

Chao, L. L., Haxby, J. V., & Martin, A. (1999). Attribute-based neural substrates in temporal cortex for perceiving and knowing about objects. *Nature Neuroscience, 2*(10), 913–919.

Chao, L. L., & Martin, A. (2000). Representation of manipulable man-made objects in the dorsal stream. *Neuroimage, 12*(4), 478–484.

Chen, J., Snow, J. C., Culham, J. C., & Goodale, M. A. (2017). What role does "elongation" play in "tool-specific" activation and connectivity in the dorsal and ventral visual streams? *Cerebral Cortex*, 1–15.

Choi, S., Na, D. L., Kang, E., Lee, K., Lee, S., & Na, D. (2001). Functional magnetic resonance imaging during pantomiming tool-use gestures. *Experimental Brain Research, 139*(4), 311–317.

Choi, H.-J., Zilles, K., Mohlberg, H., Schleicher, A., Fink, G. R., Armstrong, E., et al. (2006). Cytoarchitectonic identification and probabilistic mapping of two distinct areas within the anterior ventral bank of the human intraparietal sulcus. *Journal of Computational Neurology, 495*(1), 53–69.

Creem-Regehr, S. H., & Lee, J. N. (2005). Neural representations of graspable objects: Are tools special? *Cognitive Brain Research, 22*(3), 457–469.

Culham, J. C., & Valyear, K. F. (2006). Human parietal cortex in action. *Current Opinion in Neurobiology, 16*(2), 205–212.

Damasio, H., Grabowski, T. J., Tranel, D., Hichwa, R. D., & Damasio, A. R. (1996). A neural basis for lexical retrieval. *Nature, 380*(6574), 499–505.

Downing, P. E., Chan, A. W.-Y., Peelen, M. V., Dodds, C. M., & Kanwisher, N. (2006). Domain specificity in visual cortex. *Cerebral Cortex, 16*(10), 1453–1461.

Downing, P. E., Jiang, Y., Shuman, M., & Kanwisher, N. (2001). A cortical area selective for visual processing of the human body. *Science, 293*, 2470–2473.

Eickhoff, S. B., Paus, T., Caspers, S., Grosbras, M. H., Evans, A. C., Zilles, K., & Amunts, K. (2007). Assignment of functional activations to probabilistic cytoarchitectonic areas revisited. *Neuroimage, 36*(3), 511–521.

Ellis, P. D. (2010). Interpreting effects. In *The essential guide to effect sizes statistical power, meta-analysis, and the interpretation of research results* (pp. 31–44).

Fabbri, S., Stubbs, K. M., Cusack, R., & Culham, J. C. (2017). Disentangling representations of object and grasp properties in the human brain. *The Journal of Neuroscience, 36*(29), 7648–7662.

Fedorenko, E., Duncan, J., & Kanwisher, N. (2013). Domain-general regions in the human brain. *Proceedings of the National Academy of Sciences, 110*(41), 16616–16621.

Freud, E., Culham, J. C., Plaut, D. C., & Behrmann, M. (2017). The large-scale organization of shape processing in the ventral and dorsal pathways. *Elife, 6*, Article e27576.

Freud, E., Ganel, T., Shelef, I., Hammer, M. D., Avidan, G., & Behrmann, M. (2017). Three-dimensional representations of objects in dorsal cortex are dissociable from those in ventral cortex. *Cerebral Cortex, 27*(1), 422–434.

Gallivan, J. P., Adam McLean, D., Valyear, K. F., & Culham, J. C. (2013). Decoding the neural mechanisms of human tool use. *eLife, 2013*(2).

Glerean, E., Pan, R. K., Salmi, J., Kujala, R., Lahnakoski, J. M., Roine, U., et al. (2016). Reorganization of functionally connected brain subnetworks in high-functioning autism. *Human Brain Mapping, 37*, 1066–1079.

Haxby, J. V., Gobbini, M. I., Furey, M. L., Ishai, A., Schouten, J. L., & Pietrini, P. (2001). Distributed and overlapping representations of faces and objects in ventral temporal cortex. *Science, 293*(5539), 2425–2430.

Hentschke, H., & Stüttgen, M. C. (2011). Computation of measures of effect size for neuroscience data sets. *European Journal of Neuroscience, 34*(12), 1887–1894.

Hermsdörfer, J., Terlinden, G., Mühlau, M., Goldenberg, G., & Wohlschläger, A. M. (2007). Neural representations of pantomimed and actual tool use: Evidence from an event-related fMRI study. *Neuroimage, 36*(suppl. 2).

Holler, D. E., Fabbri, S., & Snow, J. C. (2020). Object responses are highly malleable, rather than invariant, with changes in object appearance. *Scientific Reports, 10*(4654).

IBM. (2013). *SPSS Statistics for Linux, Version 22.0*. Armonk, NY: IBM Corp.

Johnson-Frey, S. H. (2004). The neural bases of complex tool use in humans. *Trends in Cognitive Sciences, 8*(2), 71–78.

Kastner, S., Chen, Q., Jeong, S. K., & Mruczek, R. E. B. (2017). A brief comparative review of primate posterior parietal cortex: A

novel hypothesis on the human toolmaker. *Neuropsychologia, 105*, 123–134.
Konen, C. S., & Kastner, S. (2008). Two hierarchically organized neural systems for object information in human visual cortex. *Nature Neuroscience, 11*(2), 224–231.
Konen, C. S., Mruczek, R. E., Montoya, J. L., & Kastner, S. (2013). Functional organization of human posterior parietal cortex: Grasping- and reaching-related activations relative to topographically organized cortex. *Journal of Neurophysiology, 109*(12), 2897–2908.
Koski, L., Iacoboni, M., & Mazziotta, J. C. (2002). Deconstructing apraxia: Understanding disorders of intentional movement after stroke. *Current Opinion in Neurology, 15*(1), 71–77.
Kourtis, D., Vandemaele, P., & Vingerhoets, G. (2018). Concurrent cortical representations of function- and size-related object affordances: An fMRI study. *Cognitive, Affective & Behavioral Neuroscience, 18*, 1221–1232.
Kriegeskorte, N., & Mur, M. (2012). Inverse MDS: Inferring dissimilarity structure from multiple item arrangements. *Frontiers in Psychology, 3*, 245.
Kriegeskorte, N., Mur, M., Ruff, D. A., Kiani, R., Bodurka, J., Esteky, H., et al. (2008). Matching categorical object representations in inferior temporal cortex of man and monkey. *Neuron, 60*(6), 1126–1141.
Leiguarda, R. C., & Marsden, C. D. (2000). Limb apraxias: Higher-order disorders of sensorimotor integration. *Brain : A Journal of Neurology, 123*(Pt 5), 860–879.
Lewis, J. W. (2006). Cortical networks related to human use of tools. *Neuroscientist, 12*(3), 211–231.
Macdonald, S. N., & Culham, J. C. (2015). Do human brain areas involved in visuomotor actions show a preference for real tools over visually similar non-tools? *Neuropsychologia, 77*, 35–41.
Maravita, A., & Iriki, A. (2004). Tools for the body (schema). *Trends in Cognitive Sciences, 8*(2), 79–86.
MATLAB. (2018b). *MATLAB*. Natick, Massachusetts, United States: The MathWorks, Inc.
Moll, J., de Oliveira-Souza, R., Passman, L. J., Cimini Cunha, F., Souza-Lima, F., & Andreiuolo, P. A. (2000). Functional MRI correlates of real and imagined tool-use pantomimes. *Neurology, 54*(6), 1331–1336.
Mruczek, R. E. B., von Loga, I. S., & Kastner, S. (2013). The representation of tool and non-tool object information in the human intraparietal sulcus. *Journal of Neurophysiology, 109*(12), 2883–2896.
Op de Beeck, H. (2010). Against hyperacuity in brain reading: Spatial smoothing does not hurt multivariate fMRI analyses? *NeuroImage, 49*(3), 1943–1948.
Peeters, R., Simone, L., Nelissen, K., Fabbri-Destro, M., Vanduffel, W., Rizzolatti, G., et al. (2009). The representation of tool use in humans and monkeys: Common and uniquely human features. *Journal of Neuroscience, 29*(37), 11523–11539.
Perini, F., Caramazza, A., & Peelen, M. V. (2014). Left occipitotemporal cortex contributes to the discrimination of tool-associated hand actions: fMRI and TMS evidence. *Frontiers in Human Neuroscience, 8*.
Proklova, D., Kaiser, D., & Peelen, M. V. (2016). Disentangling representations of object shape and object category in human visual cortex: the Animate–Inanimate Distinction. *Journal of Cognitive Neuroscience, 28*, 680–692.
Randerath, J., Goldenberg, G., Spijkers, W., Li, Y., & Hermsdörfer, J. (2010). Different left brain regions are essential for grasping a tool compared with its subsequent use. *Neuroimage, 53*(1), 171–180.
Rice, G. E., Watson, D. M., Hartley, T., & Andrews, T. J. (2014). Low-level image properties of visual objects predict patterns of neural response across category-selective regions of the ventral visual pathway. *Journal of Neuroscience, 34*(26), 8837–8844.
Richter, M., Amunts, K., Mohlberg, H., Bludau, S., Eickhoff, S. B., Zilles, K., et al. (2019). Cytoarchitectonic segregation of human posterior intraparietal and adjacent parieto-occipital sulcus and its relation to visuomotor and cognitive functions. *Cerebral Cortex, 29*(3), 1305–1327.
Rumiati, R. I., Weiss, P. H., Shallice, T., Ottoboni, G., Noth, J., Zilles, K., et al. (2004). Neural basis of pantomiming the use of visually presented objects. *Neuroimage, 21*(4), 1224–1231.
Sakuraba, S., Sakai, S., Yamanaka, M., Yokosawa, K., & Hirayama, K. (2012). Does the human dorsal stream really process a category for tools? *Journal of Neuroscience, 32*(11), 3949–3953.
Tranel, D., Damasio, H., & Damasio, A. R. (1997). A neural basis for the retrieval of conceptual knowledge. *Neuropsychologia, 35*(10), 1319–1327.
Valyear, K. F., Cavina-Pratesi, C., Stiglick, A. J., & Culham, J. C. (2007). Does tool-related fMRI activity within the intraparietal sulcus reflect the plan to grasp? *Neuroimage, 36*(suppl. 2), T94–T108.
Watson, D. M., Hartley, T., & Andrews, T. J. (2014). Patterns of response to visual scenes are linked to the low-level properties of the image. *Neuroimage, 99*, 402–410.
Willenbockel, V., Sadr, J., Fiset, D., Horne, G. O., Gosselin, F., & Tanaka, J. W. (2010). Controlling low-level image properties: The SHINE toolbox. *Behavior Research Methods, 42*, 671–684.
Xu, Y. (2018). A tale of two visual systems: invariant and adaptive visual information representations in the primate brain. *Annual Review of Vision Science, 4*(1), 311–336.